Journal of Enhanced Heat Transfer, 27(3):249–266 (2020)

EXPERIMENTAL INVESTIGATIONS ON THERMAL PERFORMANCE OF DOUBLE PIPE HEAT EXCHANGER USING EG-WATER–BASED SiC NANOFLUID

T. Kanthimathi,[1,] P. Bhramara,[2] & G. Abhiram[3]*

[1]*Research Scholar, JNT University Hyderabad, Telangana State, India*
[2]*Mechanical Engineering, JNTUH College of Engineering Hyderabad, Telangana State, India*
[3]*PG Student, JNTUH College of Engineering Hyderabad, Telangana State, India*

*Address all correspondence to: T. Kanthimathi, JNT University Hyderabad, Telangana State, India, E-mail: pkanthi1978@gmail.com

Original Manuscript Submitted: 11/7/2019; Final Draft Received: 2/10/2020

The flow and heat transfer aspects of SiC nanoparticles dispersed in an ethylene glycol (EG)-water mixture in a volume ratio of 20:80 (SiC/20:80 EG-water) as the base fluid was experimentally determined under turbulent conditions using a double pipe heat exchanger (DPHE) with a U-bend. The experiments were performed at an operating temperature of 45°C for very low volume concentrations of nanofluid in the range of 0.01% to 0.08%. Significant enhancement in the thermophysical properties was obtained, even for low volume concentrations with the SiC/20:80 EG-water nanofluid. At a volume concentration of 0.08%, the enhancement percentages in thermal conductivity and viscosity were 40.63% and 38.2%, respectively. The experimental results of the heat transfer coefficient and friction factor were found to be in good agreement with that of correlations available in the literature. An average enhancement of 55.29% was obtained in the heat transfer coefficient for a 0.08% volume concentration of the SiC/20:80 EG-water nanofluid over the range of flow rates considered in the analysis. A maximum thermal performance factor (TPF) of 1.148 was obtained at a volume concentration of 0.08% and at a Reynolds Number of 9000.

KEY WORDS: *nanofluid, heat transfer coefficient, friction factor, thermal performance factor (TPF), double pipe heat exchanger (DPHE)*

1. INTRODUCTION

Progressive research in the field of nanofluids, since their introduction by Choi et al. (1995), has led to the emergence of nanofluids as new working fluids that have the potential to perform better than conventional heat transfer fluids, viz., water, ethylene glycol (EG), propylene glycol, oils, etc. The present research on nanofluids is essentially focused on the aspects of stability, the effect of the physical and operating parameters on their thermophysical properties, heat transfer enhancement, and the use of the nanofluids in various thermofluid applications.

Heris et al. (2014) experimentally determined the heat transfer behavior of car radiators using CuO/40:60 EG-water at different inlet temperatures of 35, 44, and 54°C. They performed

NOMENCLATURE

A	area (M^2)
c_p	specific heat ($J \cdot kg^{-1} \cdot K^{-1}$)
d_h	hydraulic diameter (m)
DIW	deionized water
DW	distilled water
EG	ethylene glycol
f	friction factor
h	heat transfer coefficient ($W \cdot m^{-2} \cdot K^{-1}$)
K	Boltzmann constant ($= 1.3807 \times 10^{-23}$ $J \cdot K^{-1}$)
k	thermal conductivity ($W \cdot m^{-1} \cdot K^{-1}$)
L	length of the pipe (m)
LMTD	logarithmic mean temperature difference
M	molecular weight
$\dot{m}$	mass flow rate ($kg \cdot s^{-1}$)
N_A	Avogadro number ($= 6.022 \times 10^{23}$ mol)
n	number of moles
Nu	Nusselt number
P	pressure (Pa)
Pe	Peclet number
Pr	Prandtl number
$\dot{Q}$	heat transfer rate (W)
r	radius (m)
Re	Reynolds number
T	temperature (°C)
TPF	thermal performance factor
U	overall heat transfer coefficient ($W \cdot m^{-2} \cdot K^{-1}$)
V	velocity ($m \cdot s^{-1}$)
V_m	molar volume of the nanofluid
W	weight (kg)
X	mole fraction

Greek Symbols

Δ	difference
η	thermal performance factor
λ	wavelength
μ	dynamic viscosity ($N \cdot m^2 \cdot s^{-1}$)
ρ	density ($kg \cdot m^{-3}$)
ϕ	volume concentration

Subscripts

avg	average
bf	base fluid
cf	cold fluid
ci	cold inlet
co	cold outlet
hf	hot fluid
hi	hot inlet
ho	hot outlet
i	inlet
is	inside surface
nf	nanofluid
np	nanoparticle
o	outlet
p	particle
w	water

experiments for a volume concentration range of 0.05%–0.8% with the Reynolds number varying from 2000 to 8000. They reported maximum enhancement of 55% in the heat transfer coefficient at a volume concentration of 0.8% corresponding to a Reynolds number of 8000 at the higher inlet temperature of 54°C. They concluded that these results help to develop compact radiators for cars, which in turn would decrease the weight and fuel consumption.

Subhedar et al. (2018) reported the results of experimental investigations on the heat transfer potential of 0.2% to 0.8% Al_2O_3 in 50:50 water/mono-ethylene glycol nanofluid as a car radiator coolant. The experiments were performed varying the operating temperature in the range of 65 to 85°C. The results indicated that for the range of flow rates considered in the analysis, the enhancement in the Nusselt number was reported to range from 3.89% to 28.47% as the volume

concentration increased from 0.2% to 0.8% at the different operating temperatures considered in the analysis.

Fard et al. (2019) experimentally investigated the heat transfer coefficient and friction factor of a spiral heat exchanger with three different spiral tube geometries using a multi-walled carbon nanotube and water as the nanofluid for volume concentrations of 0.1% and 0.5% under turbulent conditions. The results indicated that as the tube curvature ratio increased the friction factor and heat transfer coefficient increased, and maximum values were obtained for a coil with a curvature ratio of 0.123. They reported that the addition of nanotubes enhanced the heat transfer rate with an increase in the volume fraction.

An extensive review was conducted by Guo (2020) on heat transfer enhancement using nanofluids, in which various techniques available for measuring the thermal properties of nanofluids, applications of nanofluids, models used for heat transfer properties, and challenges and future research on nanofluids were summarized. He emphasized the need to develop robust techniques that take into consideration local weather conditions for large scale production of stable nanofluids, and indicated that most of the available research on nanofluids involves metal oxide nanoparticles although higher enhancement has been obtained for metallic nanoparticles. Guo (2020) insisted that extensive research on metallic nanoparticles at low volume concentrations is required.

Akash et al. (2019) experimentally investigated the thermohydraulic performance of a graphite/water-EG nanofluid as the coolant in a vehicle radiator. The results indicated that for low pumping power cases, the overall heat transfer coefficient of the nanocoolant was higher than that of the base fluid. They reported that the performance index was higher for the graphite coolant at lower coolant and air mass flow rates but was diminished in experiments with higher flow rates.

Nayak and Mishra (2019) experimentally investigated the heat transfer enhancement from a hot steel surface by impinging a TiO_2/water nanofluid. They conducted experiments for volume concentrations ranging from 0.01% to 0.07%. The results indicated that a nanofluid spray is more effective in heat dissipation (by 19.34%) compared with conventional water. These works demonstrate the applicability of nanofluid in diverse fields of thermal engineering.

Azmi et al. (2016a) investigated the heat transfer and friction factor of Al_2O_3 and TiO_2 in 40:60 EG-water for a volume concentration range of 0.5%–1.0% under turbulent flow conditions inside a tube. They performed experiments at different operating temperatures of 30, 50, and 70°C, and reported maximum heat transfer enhancements of 24.2% and 23.8% compared with the base fluid for the TiO_2 and Al_2O_3 nanofluids, respectively, at an operating temperature of 70°C for a volume concentration of 1%. For the same volume concentration, at 30°C the heat transfer coefficient of TiO_2 in the 40:60 EG-water nanofluid was reported to be less than that of Al_2O_3, and also that of the base fluid itself. However, with an increase in the operating temperature, the heat transfer coefficient of both fluids increased significantly compared with the base fluid. Their results showed negligible difference between the heat transfer coefficients obtained at 50°C and 70°C for both fluids at higher Reynolds numbers, which was explained as being a result of the dominant effect of turbulence over the difference in the thermophysical properties of both fluids at higher Reynolds numbers.

Kulkarni et al. (2008) investigated the effect of particle size (20, 50, and 100 nm) of SiO_2 nanoparticles on the viscosity and heat transfer coefficient using SiO_2/60:40 EG-water nanofluid for volume concentrations in the range of 2%–10% and Reynolds numbers varying from 3000 to 12,000. They found that the viscosity decreased with an increase in particle size and increased with an increase in volume concentration. The heat transfer coefficient was reported to increase

with an increase in particle size as well as particle concentration. Typical enhancement of 16% in the heat transfer coefficient was reported at 10% volume concentration for 20-nm-sized particles at a Reynolds number of 10,200. The literature presented in this section shows the effect of operating temperature, particle size, and volume concentration, and the interdependence among these parameters on the thermophysical properties and heat transfer coefficient of nanofluids.

Murshed and Castro (2016) conducted a review on the thermal conductivity and convective heat transfer characteristics of EG and EG-water–based nanofluids. They pointed out that the stability of nanoparticles is a great challenge in the preparation of nanofluids. In the case of a two-step method, the sonication time has to be properly decided in order to avoid damaging the nanoparticles, especially those with a spherical shape.

Azmi et al. (2016b) conducted a review on heat transfer augmentation using EG and EG-water–based nanofluids. They concluded that nanoparticles when used with an ethylene glycol/water mixture provide better stability in convective heat transfer investigations, and also stated that the scope for research on the effect of mixture ratio of the base fluid on the heat transfer characteristics of nanofluid. Most of the researchers used EG-water as the base fluid instead of EG in order to reduce the viscosity, and thereby enhance the heat transfer performance. The EG-water mixture has several applications in engineering, automotive, transportation, solar, and electronic cooling. In the present work, the 20:80 EG-water solution is considered as the base fluid in order to obtain stable dispersions, without compromising its heat transfer aspects, since the thermal conductivity of the EG-water mixture decreases with an increase in the volume concentration of ethylene glycol.

Huminic et al. (2017) experimentally investigated the effect of surfactant on the thermophysical properties of SiC/water nanofluid for volume concentrations of 0.5% and 1% in the temperature range of 20–50°C. The thermal conductivity was observed to decrease, whereas the viscosity and surface tension were observed to increase with an increase in the surfactant concentration in water. The thermal conductivity ratio and dynamic viscosity ratio of the nanofluid dispersed with the surfactant were not found to be affected by temperature.

Lee et al. (2011) measured the viscosity and thermal conductivity of SiC/deionized water (DIW) nanofluid in the volume concentration range of 0.001%–3%. They reported that the pH level of the nanofluid needs to be adjusted in order to obtain a stable nanofluid, and that a pH level of 11 resulted in a stable nanofluid for the combination of nanoparticles and base fluid considered in their analysis. The viscosity of the nanofluid was measured with a decreasing temperature range from 72°C to 28°C. The results indicated that the relative viscosity of 3% SiC/DIW increased from 68% to 102% for the temperature range considered. The increase in the relative thermal conductivity was reported to be 7.2% at 23°C for a 3% volume concentration compared with the base fluid.

Setia et al. (2013) discussed different methods to obtain stable nanofluids, which were prepared using a two-step method, viz., high shear homogenization, sonication, varying the pH level, and addition of surfactants. They also discussed different methods to evaluate the stability of nanofluids.

Kole and Dey (2012) studied the effect of prolonged sonication on the thermal conductivity of ZnO/ethylene glycol nanofluid. They concluded that the thermophysical properties are affected by the sonication time.

Li et al. (2016) experimentally determined the thermophysical properties of SiC/40:60 EG-water nanofluid for volume concentrations of 0%–0.5% in the temperature range of 10–50°C. They reported maximum enhancement of 53.81% in the thermal conductivity compared to that of the base fluid, at a temperature 50°C for a volume concentration of 0.5%. They reported

that the reason for the enhanced thermal conductivity at higher volume concentrations is due to increased agglomeration and increased Brownian motion with the increase in temperature. The viscosities of SiC/40:60 EG-water nanofluid were reported to be 22.46% and 18.96% higher than that of the base fluid at temperatures of 50°C and 10°C, respectively, for a volume concentration of 0.5%.

Yu et al. (2009) performed experiments to determine the heat transfer coefficient with water-based SiC nanofluids at 3.7% volume concentration with the Reynolds number varying from 3300 to 13,000. The results indicated that the enhancement in the heat transfer coefficient was 50%–60% above the base fluid for the range of Reynolds number considered.

Nikkam et al. (2014) investigated the heat transfer characteristics of α-SiC nanofluid at volume concentrations of 3%, 6%, and 9% using distilled water (DW) and 50:50 EG-DW (50:50) at an operating temperature of 20°C in the laminar flow regime with the Reynolds number varying from 500 to 1800. The highest enhancement in the heat transfer coefficient was reported to be 5.5% compared to that of the base fluid, for a volume concentration of 9% EG-water–based α-SiC nanofluid at a Reynolds number of 1800. They reported that the EG-water–based nanofluid exhibited better heat transfer characteristics than the water-based nanofluid.

Timofeeva et al. (2011) experimentally investigated the thermal conductivity, viscosity, and heat transfer coefficient of SiC/50:50 EG-water at 4% volume concentration for particle sizes varying from 16 to 90 nm at bulk temperatures of 51, 61, and 71°C, and the results were compared with SiC/water nanofluid for the same volume concentration and particle size. The thermal conductivity enhancement compared to the base fluid was reported to be 4% to 5% higher for SiC/water for the same volume concentration and particle size. The viscosity of the nanofluid was reported to decrease with an increase in particle size. The difference in the increase in the viscosity ratio was observed to be more pronounced with a decrease in the particle size. With an increase in the temperature, higher enhancement in the heat transfer coefficient was reported at the same volume concentration and particle size. Similarly, with an increase in the particle size, the heat transfer coefficient was reported to increase at the same operating temperature and volume concentration.

SiC nanoparticles are environmentally neutral and have minimum risk associated with their disposal. Thus, the choice of SiC in 20:80 EG-water–based fluids in the present work is driven by environmental concerns. A mixture of 20:80 EG-water in combination with very low volume concentrations of up to 0.08% of SiC nanoparticles is the scope of this research since there is limited literature published regarding this combination.

2. PREPARATION OF THE NANOFLUIDS

The two-step method was used to prepare the SiC/20:80 EG-water nanofluid. Nanoparticles of less than 50 nm size and with 99% purity were procured from Nano Amor USA Texas. The mass of the nanoparticles for a particular volume concentration was calculated using Eq. (1):

$$\phi = \frac{W_{\mathrm{np}}/\rho_{\mathrm{np}}}{(W_{\mathrm{np}}/\rho_{\mathrm{np}}) + (W_{\mathrm{bf}}/\rho_{\mathrm{bf}})} \times 100 \tag{1}$$

where np denotes nanoparticle and bf denotes base fluid.

The SiC nanoparticles were dispersed in the base fluid using a mechanical stirrer. The nanofluid was stirred continuously for about 36 to 48 hours to obtain a stable solution that lasted for approximately 32 to 48 hours for the range of volume concentrations considered in the analysis.

3. EXPERIMENTAL METHODS

3.1 Measurement of Viscosity and Thermal Conductivity

The viscosity of the SiC/20:80 EG-water nanofluid was measured using a DV3T Rheometer. An ultrasonic interferometer was used to measure the thermal conductivity of the SiC/20:80 EG-water nanofluid. This apparatus measures the velocity of an ultrasonic wave in nanofluids in order to study the effect of temperature on velocity in nanofluids at different concentrations. The nanofluid interferometer generates sound waves in nanofluids with diverse concentrations at dissimilar temperatures. These waves of known frequency are produced by a piezoelectric transducer and the wavelength is measured using a digital micrometer.

Equation (2) was used to calculate the thermal conductivity of the SiC/20:80 EG-water nanofluid at different concentrations:

$$k = 3 \times \left(\frac{N_A}{V_m}\right)^{2/3} \times K \times V \tag{2}$$

where N_A is the Avogadro number (6.022×10^{23} mol); V_m is the molar volume of the nanofluid; K is the Boltzmann constant (1.3807×10^{-23} J/K); and V is the velocity of the sound wave. The viscosity and thermal conductivity of nanofluids for different volume concentrations were determined at an operating temperature of 45°C.

3.2 Measurement of Density and Specific Heat

The density and specific heat of the SiC/20:80 EG-water nanofluid were estimated using Eqs. (3) and (4), respectively, given by Pak and Cho (1998):

$$\rho_{\mathrm{nf}} = (1 - \phi)\, \rho_{\mathrm{bf}} + \phi \rho_{\mathrm{p}} \tag{3}$$

$$c_{p_{\mathrm{nf}}} = \frac{(1 - \phi)\, \rho_{\mathrm{bf}} c_{p_{\mathrm{bf}}} + \phi \rho_{\mathrm{p}} c_{p_{\mathrm{p}}}}{\rho_{\mathrm{nf}}} \tag{4}$$

3.3 Experimental Setup and Procedure

The test section consisted of a double pipe heat exchanger (DPHE) with a U-bend, as illustrated in the schematic diagram of the experimental setup in Fig. 1, which shows that hot fluid flows through the inner tube and water at room temperature passes through the annulus at a constant flow rate. The inner pipe of the heat exchanger was made of stainless steel with a 19-mm inner diameter and 25-mm outer diameter. The outer pipe was made of galvanized iron with a 56-mm outer diameter and 50-mm inner diameter. The total length of the pipe was 4.52 m. The other parts of the setup included two reservoirs for hot and cold water, two 2 KW immersion heaters, a temperature controller, and a data logger for the measurement of all relevant parameters, viz., flow rate, temperature, and pressure drop.

The experimental setup was validated by comparing the experimental heat transfer coefficient of water with the Dittus (1930) and Gnielinski (1976) correlations, as given in Fig. 2, which shows that the experimental data for water is in good agreement with both the Dittus (1930) and Gnielinski (1976) correlations, with average deviations in the range of 14.25%–4.84%, respectively. After validation, the experiments were repeated with the 20:80 EG-water and SiC/20:80 EG-water nanofluids at different concentrations ranging from 0.01% to 0.08%. The flow rate

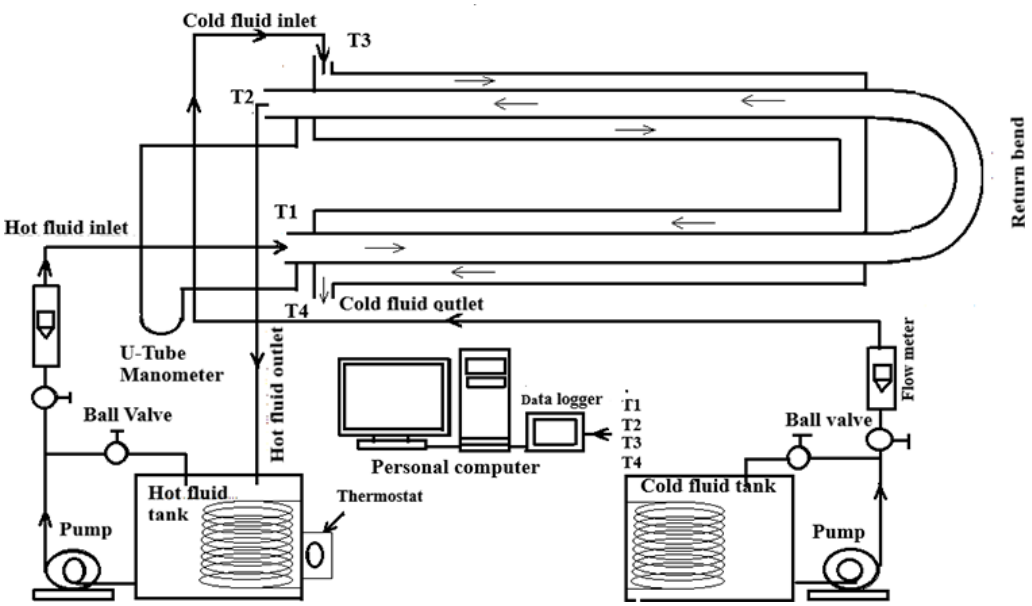

FIG. 1: Schematic diagram of a double pipe heat exchanger with a U-bend

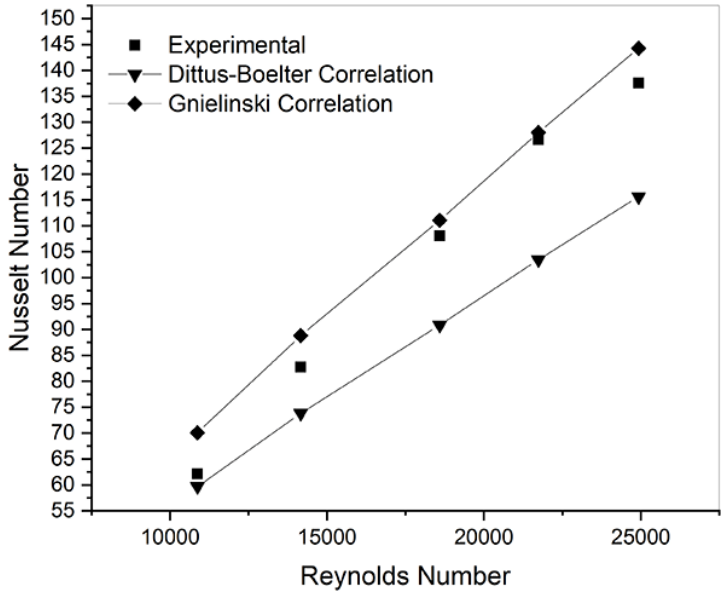

FIG. 2: Validation of the experimental setup with water

was varied from 6 to 14 l/min, in steps of 2 l/min, while maintaining a constant flow rate of cold water in the annulus.

3.4 Estimation of the Heat Transfer Coefficient

The heat lost by the hot fluid (hf) and heat gained by the cold fluid (cf) was calculated using Eqs. (5) and (6). Equation (7) gives the average heat duty of the heat exchanger:

$$\dot{Q}_{\mathrm{hf}} = \dot{m}_{\mathrm{hf}} c_{p_{\mathrm{hf}}} \left(T_{\mathrm{hi}} - T_{\mathrm{ho}}\right) \tag{5}$$

$$\dot{Q}_{\mathrm{cf}} = \dot{m}_{\mathrm{cf}} c_{p_{\mathrm{cf}}} \left(T_{\mathrm{co}} - T_{\mathrm{ci}}\right) \tag{6}$$

$$\dot{Q}_{\mathrm{avg}} = \frac{\dot{Q}_{\mathrm{hf}} + \dot{Q}_{\mathrm{cf}}}{2} \tag{7}$$

Based on the recorded temperature readings, the logarithmic mean temperature difference (LMTD) was calculated using Eq. (8):

$$\mathrm{LMTD} = \frac{\Delta T_1 - \Delta T_2}{\ln\left(\Delta T_1 / \Delta T_2\right)} \tag{8}$$

where $\Delta T_1 = T_{\mathrm{hi}} - T_{\mathrm{co}}$ and $\Delta T_2 = T_{\mathrm{ho}} - T_{\mathrm{ci}}$. Using Eqs. (7) and (8), the overall heat transfer coefficient based on the inner surface area of the inner pipe was calculated using Eq. (9):

$$U_{\mathrm{i}} = \frac{\dot{Q}_{\mathrm{avg}}}{A_{\mathrm{is}} \left(\mathrm{LMTD}\right)} \tag{9}$$

where the inside surface is denoted by is, and $A_{\mathrm{is}} = \pi d_{\mathrm{i}} l$ represents the inside surface area.

The Reynolds number for the annulus flow typically falls in the range of the transition flow. Hence, the Nusselt number for the annulus pipe was calculated using the Gnielinski (1976) correlation as presented by Eq. (10):

$$\mathrm{Nu}_{\mathrm{o}} = \frac{\left(f/8\right)\left(\mathrm{Re} - 1000\right)\mathrm{Pr}}{1 + 12.7\left(f/8\right)^{0.5}\left(\mathrm{Pr}^{2/3} - 1\right)} \tag{10}$$

where Reynolds number $\mathrm{Re} = \rho V d_h / \mu$; hydraulic diameter $d_h = d_{\mathrm{o}} - d_{\mathrm{i}}$; and Pr is the Prandtl number. Friction factor f was calculated using Petukhov's (1970) equation as given by Eq. (11):

$$f = \left[0.79 \ln\left(\mathrm{Re}\right) - 1.64\right]^{-2} \tag{11}$$

Using Eq. (10), the annulus heat transfer coefficient was calculated by Eq. (12):

$$h_{\mathrm{o}} = \frac{\mathrm{Nu}_{\mathrm{o}} \times k_{\mathrm{o}}}{d_h} \tag{12}$$

Equation (13) shows the calculation of the heat transfer coefficient of the hot fluid using Eqs. (9) and (12):

$$\frac{1}{h_{\mathrm{i}}} = \frac{1}{U_{\mathrm{i}}} - \frac{r_{\mathrm{i}}}{k} \ln\left(\frac{r_{\mathrm{o}}}{r_{\mathrm{i}}}\right) - \frac{1}{h_{\mathrm{o}}} \tag{13}$$

where k is the thermal conductivity of the inner tube; r_{i} is the inner radius of the inner tube; and r_{o} is the outer radius of the inner tube.

3.5 Estimation of the Friction Factor

The friction factor of the inner tube was calculated based on the experimentally determined pressure drop across the inner tube using Eq. (14):

$$f = \frac{2\Delta P d}{\rho L V^2} \tag{14}$$

where ΔP is the pressure drop of the inner pipe; d is the inner diameter; L is the length of the pipe; V is the velocity of flow; and ρ is the density of the hot fluid.

Uncertainty in the estimation of the heat transfer coefficient and friction factor was determined based on the measurement errors in the temperature, flow rate, and pressure drop as per the procedure reported in detail in Azmi et al. (2016a). Accordingly, the uncertainty in the measurement was obtained as 0.7457% for the heat transfer coefficient and 0.01% for the pressure drop.

4. RESULTS AND DISCUSSION

4.1 Viscosity and Thermal Conductivity of the SiC/20:80 EG-Water Nanofluid

Figure 3 shows the variations in the viscosity of the SiC/20:80 EG-water nanofluid with the volume concentration at an operating temperature of 45°C. The viscosity of the nanofluid increased with the volume concentration since the number of nanoparticles per unit volume of the fluid increased with an increase in the volume concentration of the nanofluid, thus offering more resistance to the flow. The percentage of increase in the viscosity varied from 8.98% to 38.2% compared to that of base fluid since the volume concentration varied from 0.01% to 0.08% at the operating temperature of 45°C.

The thermal conductivity of the SiC nanofluid in 20:80 EG-water had a higher value than that of base fluid at all volume concentrations considered in the analysis at the operating temperature of 45°C, as shown in Fig. 4. The increase in the thermal conductivity of the base fluid due to

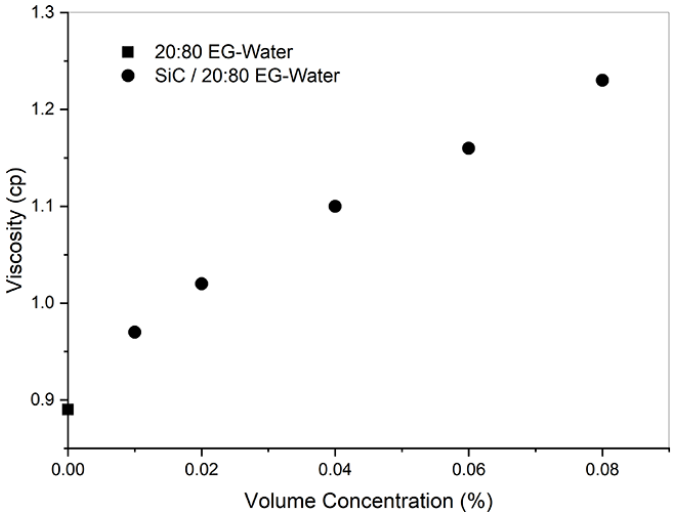

FIG. 3: Viscosity of SiC/20:80 EG-water

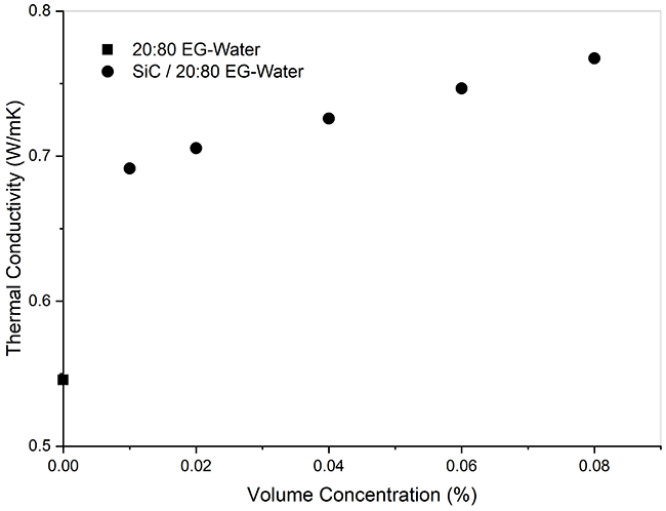

FIG. 4: Thermal conductivity of SiC/20:80 EG-water

the addition of nanoparticles is attributed to multiple factors, as stated by Machrafi and Lebon (2016), viz., liquid interfacial layering, agglomeration of nanoparticles, and Brownian motion. A maximum enhancement of 40.63% was observed in the thermal conductivity of 0.08% of the SiC/20:80 EG-water nanofluid. Even at a very low volume concentration of 0.01%, enhancement of 26.74% was obtained in the thermal conductivity of the SiC/20:80 EG-water nanofluid compared to that of the base fluid.

4.2 Comparison between the Experimental Nusselt Number and the Correlations

The experimental Nusselt number of the SiC/20:80 EG-water nanofluid was compared with that of the Dittus (1930), Pak and Cho (1998), Xuan and Li (2000), Vajjha et al. (2010), and Sharma et al. (2017) correlations, given by Eqs. (15)–(19):

$$\mathrm{Nu} = 0.023\mathrm{Re}^{0.8}\mathrm{Pr}^{0.4} \tag{15}$$

$$\mathrm{Nu} = 0.021\mathrm{Re}^{0.8}\mathrm{Pr}^{0.5} \tag{16}$$

$$\mathrm{Nu} = 0.059\left(1.0 + 0.76286\emptyset_{\mathrm{p}}^{0.6886}\mathrm{Pe}^{0.001}\right)\mathrm{Pr}_{\mathrm{nf}}^{0.9238} \tag{17}$$

$$\mathrm{Nu} = 0.065\left(\mathrm{Re}^{0.65} - 60.22\right)\left(1 + 0.0169\emptyset^{0.15}\right)\mathrm{Pr}^{0.542} \tag{18}$$

$$\mathrm{Nu} = 0.023\mathrm{Re}^{0.8}\mathrm{Pr}_{\mathrm{w}}^{0.4}\left(1 + \mathrm{Pr}_{\mathrm{nf}}\right)^{-0.012}\left(1 + \emptyset\right)^{0.23} \tag{19}$$

The comparison is presented for volume concentrations of 0.02%, 0.06%, and 0.08% SiC/20:80 EG-water nanofluids in Figs. 5(a)–5(c). At the low volume concentration of 0.02%, the Xuan and Li (2000) correlation predicted the experimental data with good agreement, while with an increase in the volume concentration, the Sharma et al. (2017), Dittus (1930), and Pak and Cho (1998) correlations predicted the experimental data well, with an average deviation of less than 15%. The Vajjha et al. (2010) correlation, in general, resulted in a comparatively higher deviation of 23.4%, as shown in Figs. 5(a)–5(c). The average deviations of the Dittus (1930), Pak and Cho (1998), Xuan and Li (2000), and Sharma et al. (2017) correlations compared with

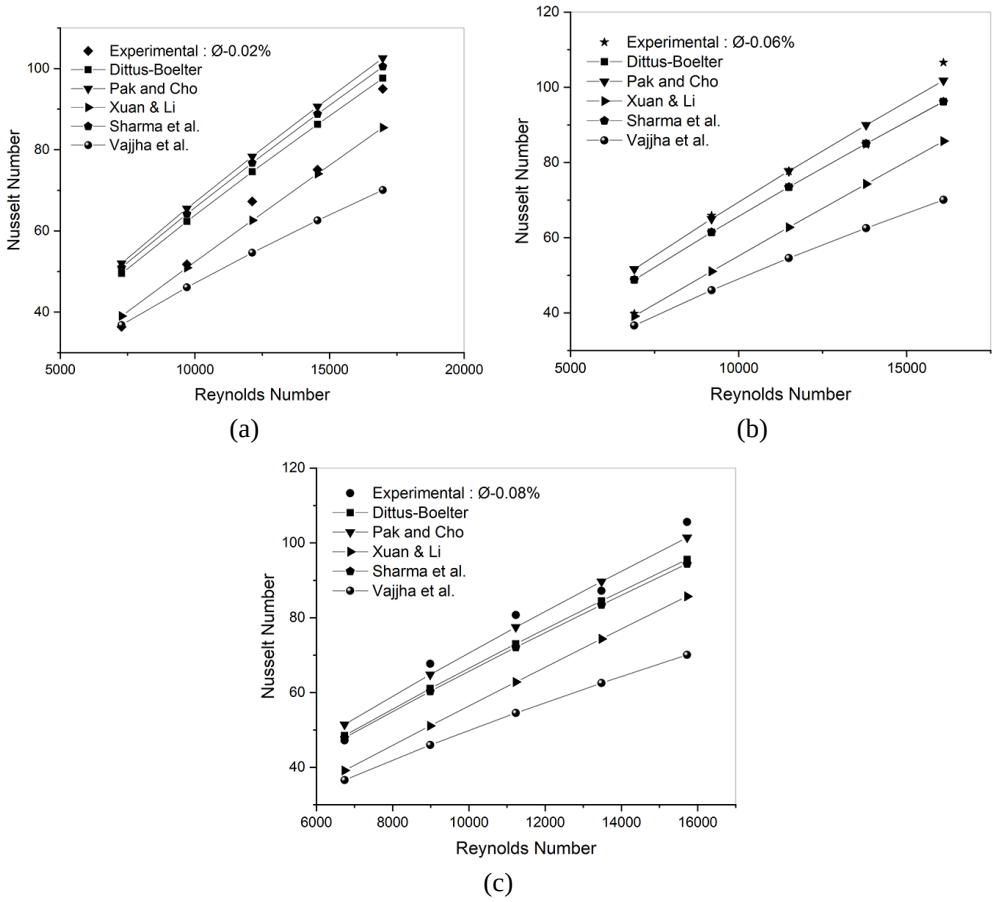

FIG. 5: Comparison between the experimental Nusselt number and the correlations at 0.02% (a), 0.06% (b), and 0.08% (c)

the experimental data, for the range of volume concentrations considered in the analysis, were observed to be 10.97%, 12.02%, 13.32%, and 12.34%, respectively.

4.3 Comparison between the Friction Factor and the Correlations

The experimental friction factor of the SiC/20:80 EG-water nanofluid was compared with that of the Vajjha et al. (2010) and Sharma et al. (2017) correlations, given by Eqs. (20) and (21), respectively:

$$f_{\mathrm{nf}} = f_{\mathrm{bf}} \left[\left(\rho_{\mathrm{nf}} / \rho_{\mathrm{bf}} \right)^{0.797} \left(\mu_{\mathrm{nf}} / \mu_{\mathrm{bf}} \right)^{0.108} \right] \tag{20}$$

$$f_{\mathrm{nf}} = f_{\mathrm{bf}} \left[\left(\rho_{\mathrm{nf}} / \rho_{\mathrm{bf}} \right)^{1.3} \left(\mu_{\mathrm{nf}} / \mu_{\mathrm{bf}} \right)^{0.3} \right] \tag{21}$$

Figures 6(a)–6(c) show the comparison of the experimental friction factor of the 0.02%, 0.06%, and 0.08% SiC/20:80 EG-water nanofluids, respectively. The average deviations of the Vajjha et al. (2010) and Sharma et al. (2017) correlations with that of the experimental friction

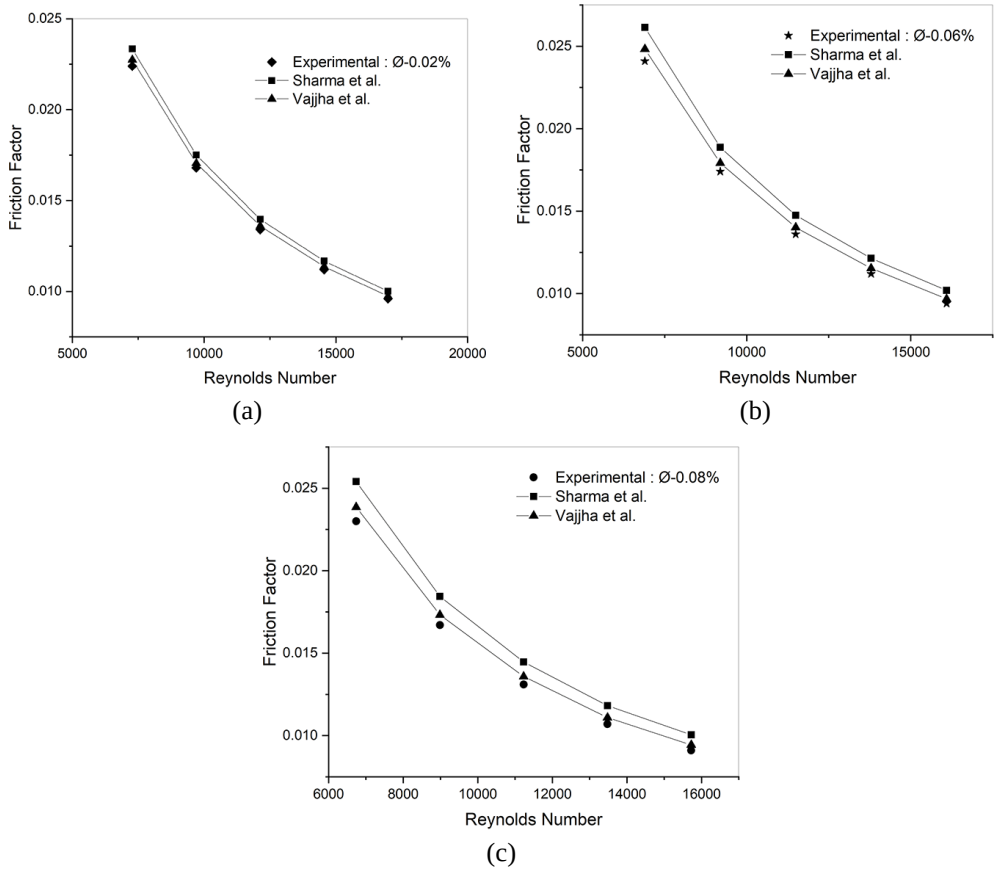

FIG. 6: Comparison between the experimental friction factor and the correlations at 0.02% (a), 0.06% (b), and 0.08% (c)

factor were observed to be 2.73% and 7.69%, respectively. This shows that at all of the volume concentrations considered in the analysis, the correlations have predicted the experimental data with good agreement.

4.4 Nusselt Number and Heat Transfer Coefficient of the SiC/20:80 EG-Water Nanofluids

Table 1 presents the thermophysical properties of the nanofluid. The enhancement in the thermophysical properties of the SiC/20:80 EG-water nanofluid was reflected in the thermal performance of the heat exchanger. Figure 7 shows the variation of the Nusselt number of the SiC/20:80 EG-water nanofluid with the Reynolds number. For the same flow rate, there was a significant decrease in the value of the Reynolds number of the SiC/20:80 EG-water nanofluid compared to that of the base fluid. This was due to an increase in the viscosity of the EG-water solution with the dispersion of SiC nanoparticles. However, the variation in the Reynolds number with the volume concentration was only marginal due to the very low volume concentrations considered

TABLE 1: Enhancement in the viscosity and thermal conductivity of the SiC/20:80 EG-water nanofluid

Volume Concentration (%)	Increase in Viscosity (%)	Increase in Thermal Conductivity (%)
0.01	8.98	26.74
0.02	14.6	29.28
0.04	23.59	33.02
0.06	30.33	36.84
0.08	38.2	40.63

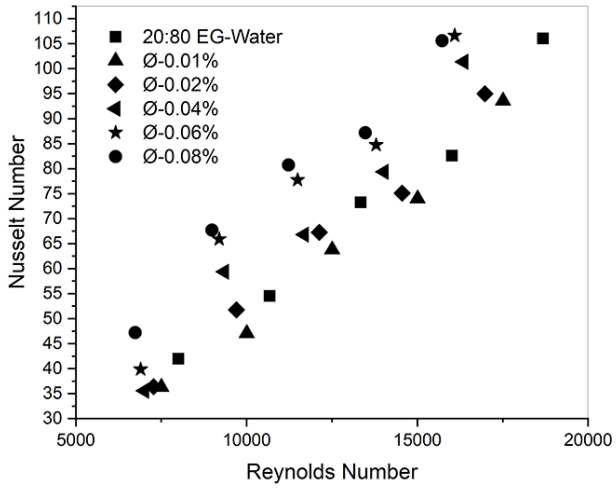

FIG. 7: Nusselt number of the SiC/20:80 EG-water nanofluid

in the analysis. At very low volume concentrations of 0.01% and 0.02% of the SiC/20:80 EG-water nanofluid, the average Nusselt number was observed to decrease by 12.93% and 8.87%, respectively, compared to that of the base fluid. For a volume concentration of 0.04% and upward, the Nusselt number started to increase by a small percentage of 4.82% and was enhanced up to 20.92% for the 0.08% volume concentration. The Nusselt number represents the number of folds by which the heat transfer is enhanced by convection from that by conduction, due to the bulk fluid movement of the fluid. The lower values of the Nusselt number compared to that of the base fluid shows that the heat transfer by conduction is dominant in the SiC/20:80 EG-water nanofluid, due to nanoparticle-induced Brownian motion and agglomeration of nanoparticles. The decrease in the Nusselt number up to the 0.02% volume concentration and the small increase in the Nusselt number from 0.04% of the nanofluid compared to that base fluid is indicates that the dominant mode of heat transfer in the SiC/20:80 EG-water nanofluid is Brownian motion–induced conduction rather than bulk fluid motion–induced convection. In addition, there was also a decrease in the Reynolds number due to an increase in the viscosity, thus decreasing the Nusselt number further, due to convection. Therefore, the Nusselt number serves as a good indicator of heat transfer enhancement in relation to the effect of heat conduction induced by dispersed nanosized particles in a base fluid.

However, due to the variation of the Reynolds number, the representation of the variation of the Nusselt number with the Reynolds number does not appear to be a suitable means of comparing the thermal performance of different nanofluids. Similar observations were reported by Timofeeva et al. (2011) and Azmi et al. (2016a). Accordingly, Timofeeva et al. (2011) noted that the Nusselt number is the best parameter to use when comparing experimental and predicted data for the same fluid and heat transfer coefficient in relation to the performance of nanofluids and base fluids having different thermal conductivities.

Figure 8 shows comparative variations of the heat transfer coefficient of the SiC/20:80 EG-water nanofluid with that of the base fluid at the different flow rates considered in the analysis, where a steady increase in the heat transfer coefficient with an increase in the volume concentration and volume flow rate can be observed. With the use of the nanofluid, the heat duty of the DPHE increases for the same flow rate and same bulk temperature of the fluid at the inlet. Thus, the increase in the heat transfer coefficient of the nanofluid is due to the increase in the overall heat transfer coefficient of the heat exchanger compared to that of the base fluid. The average increases in heat transfer coefficient were 10.98% at 0.01%, 17.47% at 0.02%, 26.82% at 0.04%, 43.73% at 0.06%, and 55.29% at 0.08% of the nanofluid, compared to that of the base fluid at the operating temperature of 45°C, over the range of flow rates considered in the analysis.

4.5 Friction Factor of the SiC/20:80 EG-Water Nanofluid

The friction factor of the SiC/20:80 EG-water nanofluid, as well as that of the base fluid, decreased with the Reynolds number, as shown in Fig. 9. The decrease in the rate of shear of the fluid within the boundary layer with an increase in the Reynolds number caused a decrease in the friction factor. For all of the volume concentrations considered in the analysis, the friction factor of the nanofluid was higher than that of the base fluid, due to an increase in the viscosity of the nanofluid with an increase in the volume concentration. However, at higher Reynolds numbers, the friction factor of the nanofluid at all of the concentrations was observed to be almost the same as that of the base fluid. This shows that at higher Reynolds numbers turbulence plays a

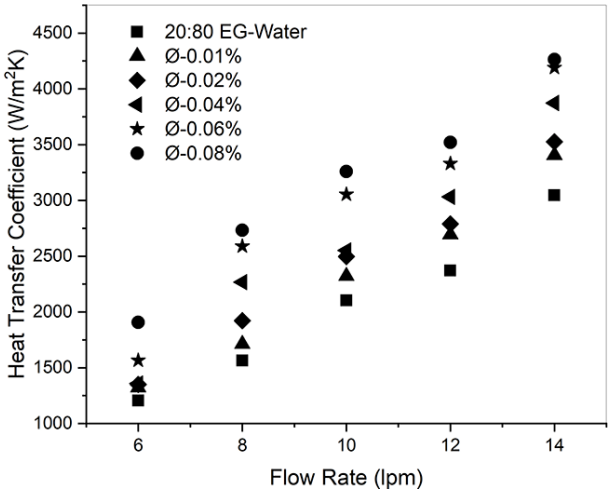

FIG. 8: Experimental heat transfer coefficient of the SiC/20:80 EG-water nanofluid with the flow rate

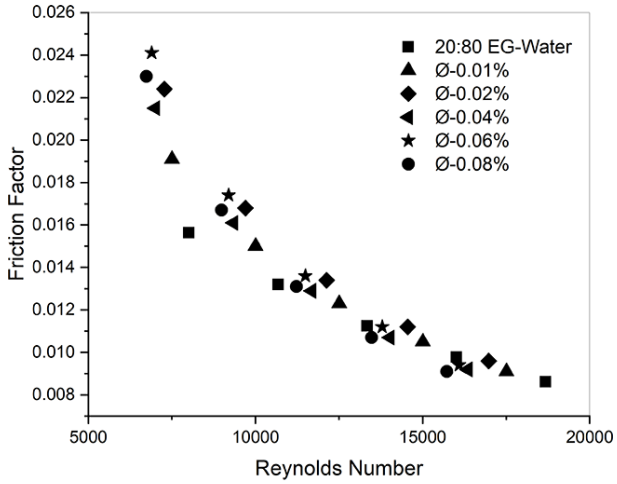

FIG. 9: Friction factor of the SiC/20:80 EG-water nanofluid with the Reynolds number

major role in the determination of the friction factor rather than the difference in the thermo-physical properties of different volume concentrations of the nanofluid. The average increase in the friction factor for the SiC/20:80 EG-water nanofluid compared to that of base fluid varied from 10.21% to 20.46% as the volume concentration was varied from 0.01% to 0.08%.

4.6 Pressure Drop of the SiC/ 20:80 EG-Water Nanofluid

Figure 10 shows the variation of the pressure drop of the nanofluid with the flow rate since the pressure drop is the direct indicator of the pumping power requirement. The pressure drop of the SiC/20:80 EG-water nanofluid increased with an increase in the volume concentration. The average increases in the pressure drop were 12.29% at 0.01%, 28.54% at 0.02%, 22.27% at

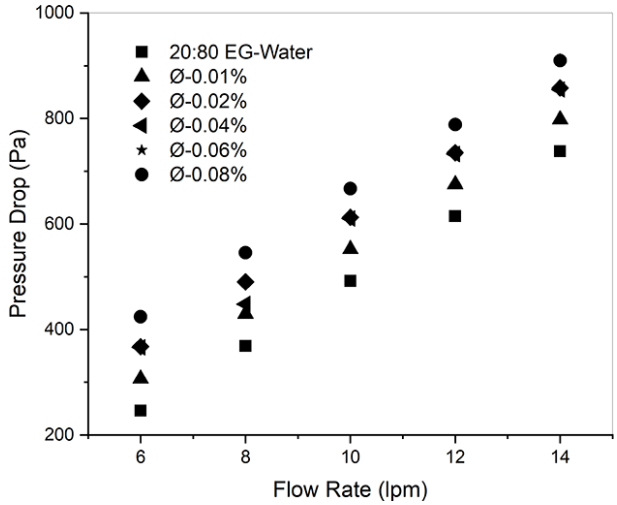

FIG. 10: Pressure drop of the SiC/20:80 EG-water nanofluid with the flow rate

0.04%, 28.56% at 0.06%, and 41.51% at 0.08% of the nanofluid compared to that of the base fluid. To determine the relative effect of the heat transfer enhancement and pressure drop penalty, the thermal performance factor (η) was calculated using Eq. (22):

$$\eta = \frac{\mathrm{Nu_{nf}}/\mathrm{Nu_{bf}}}{\left(f_{\mathrm{nf}}/f_{\mathrm{bf}}\right)^{1/3}} \tag{22}$$

Zarringhalam et al. (2016) reported that the thermal performance factor (TPF) determines the acceptability of the nanofluid in practical applications. A TPF of above 1 represents the usefulness of the working fluid in heat transfer applications with only a marginal pressure drop penalty. Figure 11 indicates the TPF of the SiC/20:80 EG-water nanofluid at the different volume concentrations considered in the analysis. The TPF was observed to increase with an increase in the volume concentration of the nanofluid. For lower volume concentrations, in the range of 0.01% to 0.04%, the TPF was observed to be below 1, while for volume concentrations of 0.06% and 0.08%, the TPF was above 1. A maximum TPF of 1.148 resulted in a volume concentration of 0.08% at a Reynolds number of 9000. These results show that the SiC/20:80 EG-water nanofluid makes a good working fluid for volume concentrations of 0.06% and 0.08%. However, with heat transfer enhancement of 17.47%, even at a low volume concentration of 0.02%, the SiC/20:80 EG-water nanofluid serves as a good heat transfer fluid.

5. CONCLUSIONS

The heat transfer and flow aspects of the SiC/20:80 EG-water nanofluid were experimentally analyzed in a DPHE for very low volume concentrations in the range of 0.01%–0.08% at the operating temperature of 45°C. The following inferences can be drawn from the analysis:

- At very low volume concentrations of up to 0.08%, significant enhancement of the thermophysical properties is observed for the SiC/20:80 EG-water nanofluid.

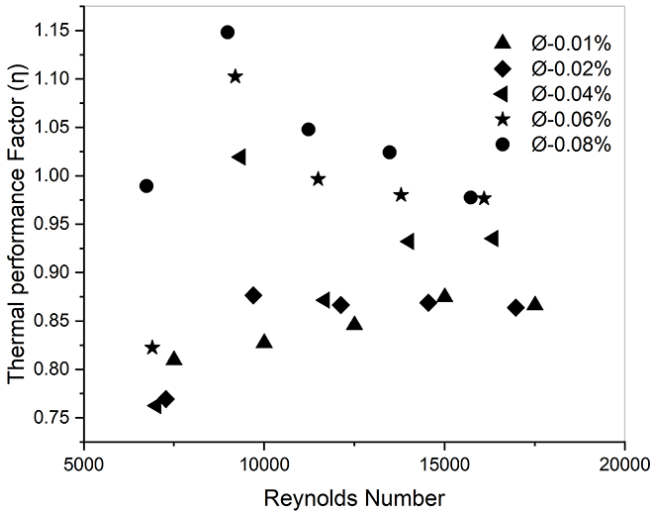

FIG. 11: Thermal performance factor of the SiC/20:80 EG-water nanofluid

- The correlations available in the literature for the Nusselt number and friction factor of nanofluids have predicted the experimental data with good agreement; in particular, the Sharma et al. (2017) and Vajjha et al. (2010) correlations.
- For the volume concentrations of the SiC/20:80 EG-water nanofluid considered in the analysis, the enhancement in the heat transfer was predominantly due to Brownian motion–induced heat conduction compared to that of bulk fluid motion–induced convection.
- An average enhancement of 55.29% in the heat transfer coefficient was obtained with the 0.08% SiC/20:80 EG-water nanofluid, thus presenting the excellent heat transfer aspects of the SiC/20:80 EG-water nanofluid as a working fluid, even at low volume concentrations of less than 0.1%.
- With the TPF value above 1, the SiC/20:80 EG-water nanofluid is proven to be a good working fluid, even for low volume concentrations of 0.06% and 0.08%.
- For the volume concentrations considered in the analysis, the maximum thermal performance factor obtained was 1.148 for a volume concentration of 0.08% of the SiC/20:80 EG-water at a Reynolds number of 9000.

REFERENCES

Akash, A.R., Pattamatta, A., and Das, S.K., Experimental Study of the Thermohydraulic Performance of Water/Ethylene Glycol–Based Graphite Nanocoolant in Vehicle Radiators, *J. Enhanced Heat Transf.*, vol. **26**, pp. 345–363, 2019.

Azmi, W.H., Hamid, K.A., Usri, N.A., Mamat, R., and Mohamad, M.S., Heat Transfer and Friction Factor of Water and Ethylene Glycol Mixture based TiO_2 and Al_2O_3 Nanofluids under Turbulent Flow, *Int. Commun. Heat Mass Transf.*, vol. **76**, pp. 24–32, 2016a.

Azmi, W.H., Hamid, K.A., Usri, N.A., Mamat, R., and Sharma, K.V., Heat Transfer Augmentation of Ethylene Glycol: Water Nanofluids and Applications—a Review, *Int. Commun. Heat Mass Transf.*, vol. **75**, pp. 13–23, 2016b.

Choi, S.U.S., Singer, D.A., and Wang, H.P., Developments and Applications of Non-Newtonian Flows, *ASME Fed.*, vol. **66**, pp. 99–105, 1995.

Dittus, F.W., *Heat Transfer in Automobile Radiators of the Tubler Type*, University of California Publications in Engineering, Berkeley, CA: University of California Press, vol. **2**, pp. 443–461, 1930.

Fard, A.M., Mirjalily, S.A.A., and Ahrar, A.J., Influence of Carbon Nanotubes on Pressure Drop and Heat Transfer Rate of Water in Helically Coiled Tubes, *J. Enhanced Heat Transf.*, vol. **26**, no. 3, pp. 217–233, 2019.

Gnielinski, V., New Equations for Heat and Mass Transfer in Turbulent Pipe and Channel Flow, *Int. Chem. Eng.*, vol. **16**, no. 2, pp. 359–368, 1976.

Guo, Z., A Review on Heat Transfer Enhancement with Nanofluids, *J. Enhanced Heat Transf.*, vol. **27**, no. 1, pp. 1–70, 2020.

Heris, S.Z., Shokrgozar, M., Poorpharhang, S., Shanbedi, M., and Noie, S.H., Experimental Study of Heat Transfer of a Car Radiator with CuO/Ethylene Glycol-Water as a Coolant, *J. Dispersion Sci. Technol.*, vol. **35**, no. 5, pp. 677–684, 2014.

Huminic, G., Huminic, A., Fleaca, C., Dumitrache, F., and Morjan, I., Thermo-Physical Properties of Water–Based SiC Nanofluids for Heat Transfer Applications, *Int. Commun. Heat Mass Transf.*, vol. **84**, pp. 94–101, 2017.

Kole, M. and Dey, T.K., Effect of Prolonged Ultrasonication on the Thermal Conductivity of ZnO–Ethylene Glycol Nanofluids, *Thermochim. Acta*, vol. **535**, pp. 58–65, 2012.

Kulkarni, D.P., Namburu, P.K., Ed Bargar, H., and Das, D.K., Convective Heat Transfer and Fluid Dynamic Characteristics of SiO_2 Ethylene Glycol/Water Nanofluid, *Heat Transf. Eng.*, vol. **29**, no. 12, pp. 1027–1035, 2008.

Lee, S.W., Park, S.D., Kang, S., Bang, I.C., and Kim, J.H., Investigation of Viscosity and Thermal Conductivity of SiC Nanofluids for Heat Transfer Applications, *Int. J. Heat Mass Transf.*, vol. **54**, nos. 1-3, pp. 433–438, 2011.

Li, X., Zou, C., and Qi, A., Experimental Study on the Thermo-Physical Properties of Car Engine Coolant (Water/Ethylene Glycol Mixture Type) based SiC Nanofluids, *Int. Commun. Heat Mass Transf.*, vol. **77**, pp. 159–164, 2016.

Machrafi, H. and Lebon, G., The Role of Several Heat Transfer Mechanisms on the Enhancement of Thermal Conductivity in Nanofluids, *Continuum Mech. Thermodyn.*, vol. **28**, no. 5 pp. 1461–1475, 2016.

Murshed, S.S. and de Castro, C.N., Conduction and Convection Heat Transfer Characteristics of Ethylene Glycol based Nanofluids—a Review, *Appl. Energy*, vol. **184**, pp. 681–695, 2016.

Nayak, S.K. and Mishra, P.C., Enhanced Heat Transfer from Hot Surface by Nanofluid based Ultrafast Cooling: An Experimental Investigation, *J. Enhanced Heat Transf.*, vol. **26**, no. 4, pp. 415–428, 2019.

Nikkam, N., Haghighi, E.B., Saleemi, M., Behi, M., Khodabandeh, R., Muhammed, M., Palm, B., and Toprak, M.S., Experimental Study on Preparation and Base Liquid Effect on Thermo-Physical and Heat Transport Characteristics of α-SiC Nanofluids, *Int. Commun. Heat Mass Transf.*, vol. **55**, pp. 38–44, 2014.

Pak, B.C. and Cho, Y.I., Hydrodynamic and Heat Transfer Study of Dispersed Fluids with Submicron Metallic Oxide Particles, *Exp. Heat Transf.*, vol. **11**, no. 2, pp. 151–170, 1998.

Petukhov, B.S., Heat Transfer and Friction in Turbulent Pipe Flow with Variable Physical Properties, *Adv. Heat Transf.*, vol. **6**, pp. 503–565, 1970.

Setia, H., Gupta, R., and Wanchoo, R.K., Stability of Nanofluids, *Mater. Sci. Forum*, vol. **757**, pp. 139–149, 2013.

Sharma, K.V., Vandrangi, S.K., Kamal, S., and Minea, A.A., Experimental Studies on the Influence of Metal and Metal Oxide Nanofluid Properties on Forced Convection Heat Transfer and Fluid Flow, in *Advances in New Heat Transfer Fluids*, London: CRC Press, pp. 1–28, 2017.

Subhedar, D.G., Ramani, B.M., and Gupta, A., Experimental Investigation of Heat Transfer Potential of Al_2O_3/Water-Mono Ethylene Glycol Nanofluids as a Car Radiator Coolant, *Case Stud. Therm. Eng.*, vol. **11**, pp. 26–34, 2018.

Timofeeva, E.V., Yu, W., France, D.M., Singh, D., and Routbort, J.L., Base Fluid and Temperature Effects on the Heat Transfer Characteristics of SiC in Ethylene Glycol/H_2O and H_2O Nanofluids, *J. Appl. Phys.*, vol. **109**, no. 1, pp. 014914(1–5), 2011.

Vajjha, R.S., Das, D.K., and Kulkarni, D.P., Development of New Correlations for Convective Heat Transfer and Friction Factor in Turbulent Regime for Nanofluids, *Int. J. Heat Mass Transf.*, vol. **53**, nos. 21-22, pp. 4607–4618, 2010.

Xuan, Y. and Li, Q., Heat Transfer Enhancement of Nanofluids, *Int. J. Heat Fluid Flow*, vol. **21**, no. 1, pp. 58–64, 2000.

Yu, W., France, D.M., Smith, D.S., Singh, D., Timofeeva, E.V., and Routbort, J.L., Heat Transfer to a Silicon Carbide/Water Nanofluid, *Int. J. Heat Mass Transf.*, vol. **52**, nos. 15-16, pp. 3606–3612, 2009.

Zarringhalam, M., Karimipour, A., and Toghraie, D., Experimental Study of the Effect of Solid Volume Fraction and Reynolds Number on Heat Transfer Coefficient and Pressure Drop of CuO–Water Nanofluid, *Exp. Therm. Fluid Sci.*, vol. **76**, pp. 342–351, 2016.